Arch Appl Mech (2017) 87:1399–1410
DOI 10.1007/s00419-017-1258-5

ORIGINAL

Jun-Hyok Ri · Hyon-Sik Hong

A modified algorithm of linear matching method for limit analysis

Received: 29 November 2016 / Accepted: 25 April 2017 / Published online: 8 May 2017

Abstract Linear matching method has been widely used for the numerical analysis of limit and shakedown. It has been proved theoretically that linear matching method could offer the monotonically reducing sequence of upper bound. Nevertheless, it still remains open whether linear matching method can obtain the conversed and reliable lower bound or not. Thus, an elastic compensation method is used generally for the evaluation of lower bound, but limit analysis using linear matching method and elastic compensation method needs double iterative computations. Moreover, the convergence can be checked only after the computation is finished because linear matching method and elastic compensation method cannot be performed simultaneously. From this, we propose a simple method in order to improve the numerical solution of lower bound by linear matching method. The Young's modulus varying spatially is determined in every iteration such that not only the stress state lies on the yielding surface but also the strain state does not exceed a certain value of reference strain, leading to the evaluation of lower bound based on the strain state but not the stress one. The proposed method can improve the numerical solution of lower bound by linear matching method without any affection on the upper bound. ANSYS UserMat is used for implementing the current method. The limit analysis is performed like the general elastic finite element analysis in ANSYS. Some numerical examples are considered in order to confirm the effectiveness of proposed approach. Numerical examples showed the validity and improvement of numerical accuracy of our approach. It should be mentioned that our approach can predict the lower bound and upper one simultaneously within the framework of only linear matching method without using the elastic compensation method.

Keywords Linear matching method · Elastic compensation method · Limit analysis · Finite element analysis · ANSYS UPF

1 Introduction

Conventional numerical methods in the limit and shakedown analysis are mostly based on the mathematical programming such as interior-point method or second-order cone programming (SOCP) [1,2]. Numerical methods based on the mathematical programming are successfully implemented, combining the finite element software with the optimization packages. For example, Simon and Weichert [2] used the commercial finite element software ANSYS for elastic stress computation as well as the software package IPSA for numerical optimization and compared obtained results with ones by various packages including LANCELOT, IPDCA and IPOPT.

The linear matching method (LMM) originally proposed by Ponter et al. [3,4] makes it possible to conduct the limit analysis using only finite element analysis but not using the mathematical programming. The LMM

J.-H. Ri · H.-S. Hong (✉)
Institute of Mechanics, State Academy of Sciences, Pyongyang, Democratic People's Republic of Korea
E-mail: hyonsik.hong@star-co.net.kp

of which the iterative process can be considered as the nonlinear mathematical programming in essence is a powerful method for limit analysis via the iteration of linear elastic FEAs. It has been proved theoretically that the LMM could offer a monotonically reducing sequence of upper bound.

Even though the LMM has been widely used for the limit analysis of metal structures [5–7] as well as composite materials [8–11] subjected to thermal and mechanical loading and implemented by using the finite element software such as ABAQUS [6,12] and ADINA [9], it has an important disadvantage that the lower bound computed in iterative process could not be used for the evaluation of error of upper bound.

This is due to the fact that solution of lower bound may be seriously oscillated in iteration process in spite that lower bound converges to upper one as the iteration number increases. Moreover, the evaluation of lower bound needs much of iterations for its convergence. To overcome this difficulty, Pisano et al. [9–11] proposed to use the LMM for the evaluation of upper bound and the Elastic Compensation Method (ECM) for the computation of lower bound. Nevertheless, in author's opinion, their method for obtaining the lower bound by the ECM and evaluating the upper one by LMM may be failed to compute lower bound and upper one simultaneously and to evaluate the error between lower bound and upper one in real-time in iterative process due to the difference in both algorithms. In addition, this method needs nearly the double size of computational cost.

In this paper, a simple method is proposed in order to improve the numerical solution of lower bound by the LMM. The Young's modulus varying spatially is determined in every iteration such that not only stress state lies on the yielding surface but also strain state does not exceed a certain value of reference strain, leading to the evaluation of lower bound based on strain state but not stress one. The proposed method can improve the numerical solution of lower bound by LMM without any affection on the upper bound. The lower bound newly evaluated based on the strain is always smaller than the upper bound in the iterative process and finally equal to the upper bound after sufficient numbers of iteration go on. Some numerical examples are considered in order to confirm the effectiveness of proposed approach. Numerical examples show the validity and the improvement of numerical accuracy of our approach. It should be mentioned that our approach can predict lower bound and upper one simultaneously within the framework of only the LMM without using the ECM.

This paper is organized as follows: The basic formulation of LMM and its algorithm is briefly introduced in Sect. 2. Section 3 describes a modified algorithm of LMM and proofs of some lemmas. Several numerical problems including plane problem, axisymmetric problem and three dimensional problem are illustrated in Sect. 4 for the validation of proposed approach. Finally, concluding remarks are presented in Sect. 5.

2 Linear matching method

2.1 Upper and lower bound theorem

The material is assumed to be rigid/perfectly-plastic which follows the von Mises yielding condition. It is assumed that a body occupies the volume V with the surface S where a traction is given as zero or $P \cdot p_i(\mathbf{x})$ on S_T and displacement $\bar{u}_i = 0$ is specified on $S_u (S = S_T + S_u)$. Here, P is a scalar parameter defining relative magnitude of applied load as compared with a reference load p_i. The lower and upper bound theorem of limit load can be postulated as follows, respectively [3].

Lower bound theorem

If, for the external load $P = P_{\mathrm{LB}}$, there exists a statically possible stress field σ_{ij}^* such that

$$f\left(\sigma_{ij}^*\right) \leq \sigma_y \tag{1}$$

at every point within V, then $P_{\mathrm{L}} \geq P_{\mathrm{LB}}$. Here, f is a von Mises yield function and σ_y is the uniaxial yield stress. Thus, one can know that a maximum value of P_{LB} becomes lower bound of limit load P_{L}.

Upper bound theorem

If, for the external load $P = P_{\mathrm{UB}}$, there exists a kinematically possible displacement rate field $\dot{u}_i^*$ and its corresponding strain rate field $\dot{\varepsilon}_{ij}^*$ such that

$$P_{\mathrm{UB}} \int_{S_T} p_i \dot{u}_i^* = \int_V \sigma_{ij}^{p*} \dot{\varepsilon}_{ij}^* \mathrm{d}V \tag{2}$$

where σ_{ij}^{p*} is a stress point at yield associated with $\dot{\varepsilon}_{ij}^*$, then satisfies $P_{\mathrm{L}} \leq P_{\mathrm{UB}}$. Hence, one can know that a minimum value of P_{UB} becomes upper bound of limit load P_{L}.

According to above theorems, the upper and lower bound of limit load can be extracted by reducing into the optimization problem, respectively.

2.2 Conventional linear matching method

For the LMM, the Young's modulus is changed spatially such that the stress field corresponding to a certain kind of kinetically possible strain field is placed on the yielding surface at every point of material. The Poisson's ratio is recommended to take the value close to 0.5 in order to account for the plastic incompressibility, in general [3,4]. Thus, we adopt the Poisson's ratio as 0.4999999 in this work.

The LMM algorithm could be formulated as follows [3].

- Initialization: Set $P_{\mathrm{UB}}^0 = 1$ and $E^1(\mathbf{x}) = E$.
- kth iteration:

The linear elastic analysis with the Young's modulus of $E^k(\mathbf{x})$ is performed under a load of p and as a result, σ_{ij}^k, ε_{ij}^k and u_i^k is obtained, respectively. And then, lower and upper bounds of the limit load at kth iteration are evaluated as

$$P_{\mathrm{LB}}^k = \frac{\sigma_y}{\max\left(\sigma_{\mathrm{eq}}\left(\sigma_{ij}^k\right)\right)} \tag{3}$$

$$P_{\mathrm{UB}}^k = \frac{\int_V \sigma_y \varepsilon_{\mathrm{eq}}\left(\varepsilon_{ij}^k\right) \mathrm{d}V}{\int_{S_T} p_i u_i^k \mathrm{d}S} \tag{4}$$

where σ_{eq} and $\varepsilon_{\mathrm{eq}}$ denote the equivalent stress and equivalent strain, respectively.

The E^{k+1} at $k+1$th iteration is taken as follows.

$$E^{k+1} = \frac{\sigma_y}{\varepsilon_{\mathrm{eq}}\left(\varepsilon_{ij}^k\right)} \tag{5}$$

Equation (5) gives E^{k+1} at $k+1$th iteration such that the stress field corresponding to strain field ε_{ij}^k obtained at kth iteration lies on the yielding surface.

3 A modified linear matching method

We update the Young's modulus at $k+1$th iteration as

$$\tilde{E}^{k+1} = \frac{E_{\mathrm{ref}}}{E_{\mathrm{min}}^{k+1}} E^{k+1} \tag{6}$$

where $\tilde{E}^{k+1}$ is the Young's modulus, E^{k+1} the one obtained by Eq. (5), $E_{\mathrm{min}}^{k+1} = \min(E^{k+1}(\mathbf{x}))$. E_{ref}, being an arbitrary constant, is taken as actual Young's modulus in this work, in convenience.

The lower bound at kth iteration is newly evaluated as follows but not Eq. (3).

$$\bar{P}_{\mathrm{LB}}^k = \frac{\varepsilon_y}{\max\left(\varepsilon_{\mathrm{eq}}\left(\varepsilon_{ij}^k\right)\right)} \tag{7}$$

Here, $\varepsilon_y = \sigma_y / E_{\mathrm{ref}}$.

We denote the upper and lower bounds evaluated according to Eqs. (3) and (4) by $\tilde{P}_{\mathrm{UB}}^k$ and $\tilde{P}_{\mathrm{LB}}^k$, respectively, at kth iteration of the LMM with Young's modulus computed by Eq. (6). To distinguish this LMM from the conventional one, we call $\tilde{P}_{\mathrm{UB}}^k$ and $\tilde{P}_{\mathrm{LB}}^k$ the modified upper and lower bound, respectively.

To make clear the meaning of Eq. (6), we assume two distributions of Young's modulus with $E_1(\mathbf{x})$ and $E_2(\mathbf{x}) = \alpha E_1(\mathbf{x})$ for the same structure, respectively. Here, α is a constant. Denoting the stress and strain field

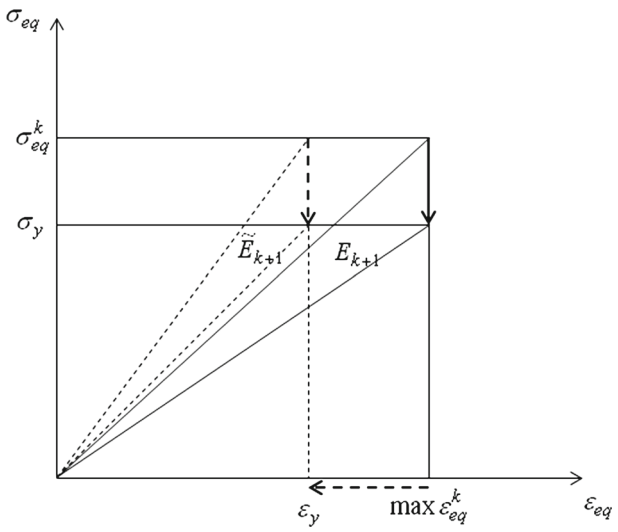

Fig. 1 Modified LMM

corresponding to $E_1(\mathbf{x})$ as σ_1 and ε_1, and $E_2(\mathbf{x}) = \alpha E_1(\mathbf{x})$ as σ_2 and ε_2, it is self-evident that one can get following relation according to the elasticity theory.

$$\sigma_2 = \sigma_1, \quad \varepsilon_2 = \frac{1}{\alpha}\varepsilon_2 \tag{8}$$

Equation (8) implies that only the strain field decreases (or increases) by α times without the change in stress field when the distribution of Young's modulus increases (or decreases) by α times. Equation (6) could be rewritten as follows.

$$\tilde{E}^{k+1} = \frac{E_{\text{ref}}}{E_{\min}^{k+1}} E^{k+1} = \frac{\max \varepsilon_{\text{eq}}^{k}}{\varepsilon_y} E^{k+1} = \alpha E^{k+1} \tag{9}$$

Equation (9) implies that our modified LMM yields the elasticity modulus $\tilde{E}^{k+1}$, being the Young's modulus E^{k+1} in the classical LMM multiplied by a certain constant. From Eqs. (9) and (8), considering expression (5) of the Young's modulus in the classical LMM, one can know that α scales the strain field obtained at kth iteration lest the equivalent strain exceeds a certain value of strain, ε_y, and that E^{k+1} makes the stress field to lie on the yielding surface for such a scaled strain field. This is shown schematically from Fig. 1.
Furthermore, from $E_{\min}^{k+1} \leq E^{k+1}$, one can get following relation.

$$\tilde{E}^{k+1} \geq E_{\text{ref}} \tag{10}$$

Based on above discussions, we can get three comments as follows.

First comment The modified upper bound and lower bound, $\tilde{P}_{\text{UB}}^{k}$ and $\tilde{P}_{\text{LB}}^{k}$, are equal to the conventional upper bound and lower one, P_{UB}^{k} and P_{LB}^{k}, respectively. Here, $\tilde{P}_{\text{UB}}^{k}$ and $\tilde{P}_{\text{LB}}^{k}$ means the upper bound and the lower one evaluated by Eqs. (4) and (3) in our modified LMM, respectively.

This comment can be proved as follows.

According to Eq. (9), the modified Young's modulus, $\tilde{E}^{k}$, is expressed as

$$\tilde{E}^{k} = \alpha E^{k}. \tag{11}$$

From Eq. (8), one can know that stress field, $\tilde{\sigma}_{ij}^{k}$, strain field, $\tilde{\varepsilon}_{ij}^{k}$, and displacement field, $\tilde{u}_{i}^{k}$, are related to the conventional σ_{ij}^{k}, ε_{ij}^{k} and u_{i}^{k} as follows.

$$\tilde{\sigma}_{ij}^{k} = \sigma_{ij}^{k}, \quad \tilde{\varepsilon}_{ij}^{k} = \frac{1}{\alpha}\varepsilon_{ij}^{k}, \quad \tilde{u}_{i}^{k} = \frac{1}{\alpha}u_{i}^{k} \tag{12}$$

Substituting the second and the third in Eq. (12) into Eq. (4), one can obtain the following expression.

$$\tilde{P}_{\mathrm{UB}}^{k}=\frac{\int_{V}\sigma_{y}\varepsilon_{\mathrm{eq}}\left(\tilde{\varepsilon}_{ij}^{k}\right)\mathrm{d}V}{\int_{S_T}p_{i}\tilde{u}_{i}^{k}\mathrm{d}S}=\frac{\int_{V}\sigma_{y}\varepsilon_{\mathrm{eq}}\left(\varepsilon_{ij}^{k}/\alpha\right)\mathrm{d}V}{\int_{S_T}p_{i}u_{i}^{k}/\alpha\mathrm{d}S}=\frac{\int_{V}\sigma_{y}\varepsilon_{\mathrm{eq}}\left(\varepsilon_{ij}^{k}\right)\mathrm{d}V}{\int_{S_T}p_{i}u_{i}^{k}\mathrm{d}S}=P_{\mathrm{UB}}^{k} \tag{13}$$

Thus, the convergence of modified upper bound, $\tilde{P}_{\mathrm{UB}}^{k}$, can be proved naturally by the convergence of upper bound in the conventional LMM.

Likewise, substituting the first in Eq. (12) into Eq. (3) yields following relation.

$$\tilde{P}_{\mathrm{LB}}^{k}=P_{\mathrm{LB}}^{k} \tag{14}$$

Second comment The newly evaluated lower bound $\bar{P}_{\mathrm{LB}}^{k}$ is smaller than or equal to the upper bound P_{UB}^{k}. This comment can be proved as follows.

According to Clapeyron's theorem of the elasticity theory, the work done by external surface traction p_i is twice the strain potential energy as great as it is [13]. Namely,

$$\int_{S_T}p_{i}u_{i}^{k}=\int_{V}\sigma_{ij}^{k}\varepsilon_{ij}^{k}\mathrm{d}V=\int_{V}\sigma_{\mathrm{eq}}^{k}\varepsilon_{\mathrm{eq}}^{k}\mathrm{d}V=\int_{V}\tilde{E}^{k}\varepsilon_{\mathrm{eq}}^{k}\varepsilon_{\mathrm{eq}}^{k}\mathrm{d}V \tag{15}$$

Substituting Eq. (15) into Eq. (4), one gets the following.

$$P_{\mathrm{UB}}^{k}=\frac{\int_{V}\sigma_{y}\varepsilon_{\mathrm{eq}}^{k}\mathrm{d}V}{\int_{V}\tilde{E}^{k}\varepsilon_{\mathrm{eq}}^{k}\varepsilon_{\mathrm{eq}}^{k}\mathrm{d}V} \tag{16}$$

Introducing $\varepsilon_{\mathrm{eq\,max}}^{k}=\max\left(\varepsilon_{\mathrm{eq}}^{k}(\mathbf{x})\right)$ and considering $\tilde{E}^{k}\geq E_{\mathrm{ref}}$ at all points according to Eq. (10), following relation can be obtained.

$$P_{\mathrm{UB}}^{k}=\frac{\int_{V}\sigma_{y}\varepsilon_{\mathrm{eq}}^{k}\mathrm{d}V}{\int_{V}\tilde{E}^{k}\varepsilon_{\mathrm{eq}}^{k}\varepsilon_{\mathrm{eq}}^{k}\mathrm{d}V}\geq\frac{\varepsilon_{y}}{\varepsilon_{\mathrm{eq\,max}}^{k}}\frac{\int_{V}E_{\mathrm{ref}}\varepsilon_{\mathrm{eq}}^{k}\mathrm{d}V}{\int_{V}\tilde{E}^{k}\varepsilon_{\mathrm{eq}}^{k}\mathrm{d}V}\geq\frac{\varepsilon_{y}}{\varepsilon_{\mathrm{eq\,max}}^{k}}\frac{\int_{V}\varepsilon_{\mathrm{eq}}^{k}\mathrm{d}V}{\int_{V}\varepsilon_{\mathrm{eq}}^{k}\mathrm{d}V}\geq\frac{\varepsilon_{y}}{\varepsilon_{\mathrm{eq\,max}}^{k}}=\bar{P}_{\mathrm{LB}}^{k} \tag{17}$$

Namely, the newly evaluated lower bound $\bar{P}_{\mathrm{LB}}^{k}$ is smaller than or equal to the upper bound P_{UB}^{k}.

In similar way, one can prove that the lower bound P_{LB}^{k} evaluated by Eq. (3) is smaller than or equal to the upper bound P_{UB}^{k}.

In fact, combining Eq. (15) with Eq. (4), following relation is obtained.

$$P_{\mathrm{UB}}^{k}=\frac{\int_{V}\sigma_{y}\varepsilon_{\mathrm{eq}}^{k}\mathrm{d}V}{\int_{V}\sigma_{\mathrm{eq}}^{k}\varepsilon_{\mathrm{eq}}^{k}\mathrm{d}V}\geq\frac{\sigma_{y}}{\max\left(\sigma_{\mathrm{eq}}^{k}\right)}\frac{\int_{V}\varepsilon_{\mathrm{eq}}^{k}\mathrm{d}V}{\int_{V}\varepsilon_{\mathrm{eq}}^{k}\mathrm{d}V}\geq\frac{\sigma_{y}}{\max\left(\sigma_{\mathrm{eq}}^{k}\right)}=P_{\mathrm{LB}}^{k} \tag{18}$$

Third comment The newly evaluated lower bound evaluated by Eq. (7) converges to P_{LB}^{k} and P_{UB}^{k} as $k\rightarrow\infty$. Namely, $\bar{P}_{\mathrm{LB}}^{k}\rightarrow P_{\mathrm{LB}}^{k}$ and $\bar{P}_{\mathrm{LB}}^{k}\rightarrow P_{\mathrm{UB}}^{k}$, $k\rightarrow\infty$.

This comment can be proved as follows.

After performing sufficient numbers of iterations, let $\varepsilon_{\mathrm{eq}}^{k-1}=\varepsilon_{\mathrm{eq}}^{k}$.

According to Eqs. (5) and (6),

$$\tilde{E}^{k}=\frac{E_{\mathrm{ref}}}{\min\frac{\sigma_{y}}{\varepsilon_{\mathrm{eq}}^{k-1}}}\cdot\frac{\sigma_{\mathrm{y}}}{\varepsilon_{\mathrm{eq}}^{k-1}}=E_{\mathrm{ref}}\frac{\max\varepsilon_{\mathrm{eq}}^{k-1}}{\varepsilon_{\mathrm{eq}}^{k-1}}=E_{\mathrm{ref}}\frac{\max\varepsilon_{\mathrm{eq}}^{k}}{\varepsilon_{\mathrm{eq}}^{k}} \tag{19}$$

$$\sigma_{\mathrm{eq}}^{k}=\tilde{E}^{k}\varepsilon_{\mathrm{eq}}^{k}=E_{\mathrm{ref}}\frac{\max\varepsilon_{\mathrm{eq}}^{k}}{\varepsilon_{\mathrm{eq}}^{k}}\varepsilon_{\mathrm{eq}}^{k}=E_{\mathrm{ref}}\max\varepsilon_{\mathrm{eq}}^{k}. \tag{20}$$

Substituting Eq. (20) into Eq. (3), one can obtain the following relation.

$$P_{\mathrm{LB}}^{k}=\frac{\sigma_{y}}{\max\sigma_{\mathrm{eq}}^{k}}=\frac{\sigma_{y}}{E_{\mathrm{ref}}\max\varepsilon_{\mathrm{eq}}^{k}}=\frac{\varepsilon_{y}}{\max\varepsilon_{\mathrm{eq}}^{k}}=\bar{P}_{\mathrm{LB}}^{k} \tag{21}$$

This means that the lower bound evaluated by Eq. (7) satisfies the lower bound theorem after performing sufficient numbers of iterations.

Meanwhile, one can easily prove that the lower bound $\bar{P}^k_{\mathrm{LB}}$ evaluated by Eq. (7) converges to the upper bound. In fact, combining Eqs. (20), (15) and (4), one can get the following relation.

$$P^k_{\mathrm{UB}} = \frac{\int_V \sigma_y \varepsilon^k_{\mathrm{eq}} \mathrm{d}V}{\int_V E_{\mathrm{ref}} \max\left(\varepsilon^k_{\mathrm{eq}}\right) \varepsilon^k_{\mathrm{eq}} \mathrm{d}V} = \frac{\sigma_y}{E_{\mathrm{ref}} \max\left(\varepsilon^k_{\mathrm{eq}}\right)} = \frac{\varepsilon_y}{\max\left(\varepsilon^k_{\mathrm{eq}}\right)} = \bar{P}^k_{\mathrm{LB}} \tag{22}$$

Therefore, the lower bound $\bar{P}^k_{\mathrm{LB}}$ satisfies the lower bound theorem and becomes the upper bound in the limit state of $\varepsilon^{k-1}_{\mathrm{eq}} = \varepsilon^k_{\mathrm{eq}}$.

4 Numerical examples

As discussed above, the LMM is based on the analysis of elastic problem considering the incompressibility with the Young's modulus varying spatially. In order to perform the elastic analysis which is necessary for the implementation of LMM, the commercially available FE code ANSYS was used in this paper. The incompressibility of material can be considered sufficiently by using the element integration technology and the element formulae in ANSYS which are appropriate for the incompressible property. The Young's modulus varying spatially can be defined by using UserMat, ANSYS subroutine. The value of Young's modulus to be used in current iteration is saved in the state variable of UserMat in the previous iteration. Once the current iteration for implementing the LMM is finished, the upper bound is evaluated by using Eq. (4) and the lower bound by using Eq. (3) or (7). Next, the analysis process is restarted in order to continue the next iteration.

4.1 Square plate with a hole in its center

The square plate with a hole in its center subjected to the uniform pressure $p = \sigma_y$ is considered as shown from Fig. 2. The limit load factor is equal to 0.8 for plane stress condition with $R/L = 0.2$. The FE model consists of 5000 PLANE182 elements and 5151 nodal points. B-bar Method (Selective Reduced Integration) is used for the element integration. Figure 3 compares the upper bound and the lower one predicted using the modified LMM with the predictions evaluated by the ECM as the iteration number increases. In this figure, solid line denotes the upper bound, dashed line represents the lower bound evaluated using Eq. (3), dotted line shows the lower bound computed using Eq. (7), and dash-dot line indicates the lower bound predicted by ECM. As seen from Fig. 3, the evaluation of lower bound by modified LMM using Eq. (7) shows the best trend of convergence. Meanwhile, the prediction of lower bound by ECM also indicates the good trend of convergence, but the convergence rate in that case is smaller than in the case using Eq. (7). Moreover, the computation of lower bound by LMM using Eq. (3) shows the convergence with local oscillations.

Figure 4 shows the relative errors of lower bound evaluated using Eq. (7) and ECM against the analytical solution of 0.8, respectively.

Necessary parameters such as stress components, strain ones and Young's modulus can be obtained at every iteration. Figure 5 shows the distribution of von Mises stress and equivalent strain evaluated at 40th iteration of modified LMM.

4.2 Single-edge cracked plate subjected to tension (SE(T))

Figure 6 shows the geometry of single-edge cracked plate under tension. Assuming plane strain condition, the width b is equal to a half of the length $2L$ and $a/b = 0.6$ as well as $b = 1$ is applied. Here, a is a crack length. Figure 7 presents FE mesh applied. The FE model consists of 7301 PLANE182 elements and 7455 nodal points. Considering the incompressibility, B-bar Method (Selective Reduced Integration) and mixed u-p formulation are used.

The analytical solution of limit load factor $\lambda = p/\sigma_y$ in plane strain condition is expressed as

$$\lambda = 1.702\gamma \left\{ \left[(0.206 - x)^2 + 0.5876(1 - x)^2 \right]^{1/2} + (0.206 - x) \right\} \quad x > 0.545 \tag{23}$$

$$\left.\begin{array}{l} \lambda \geq \gamma(1 - x - 1.232x^2 + x^3) \\ \lambda \leq \gamma\left(1 - x - 1.232x^2 + x^3 + 22x^3(0.545 - x)^2\right) \end{array}\right\} \quad x < 0.545, \tag{24}$$

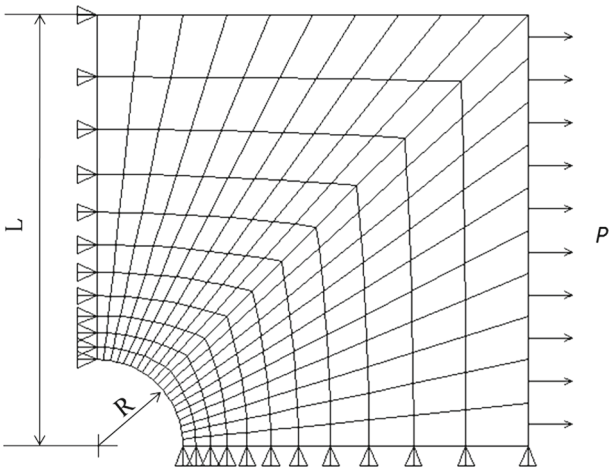

Fig. 2 Square plate with a hole in its center

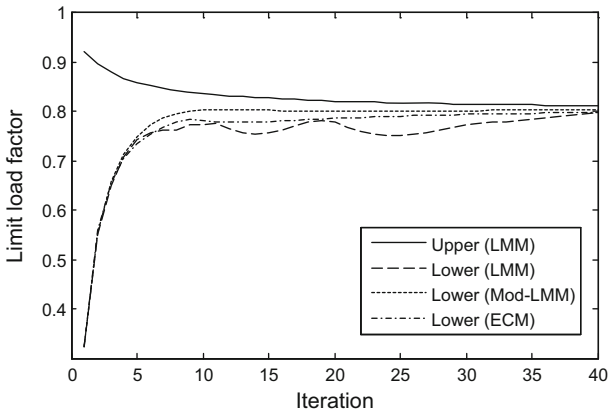

Fig. 3 Convergence process of *upper* bound and the *lower* one versus iteration number

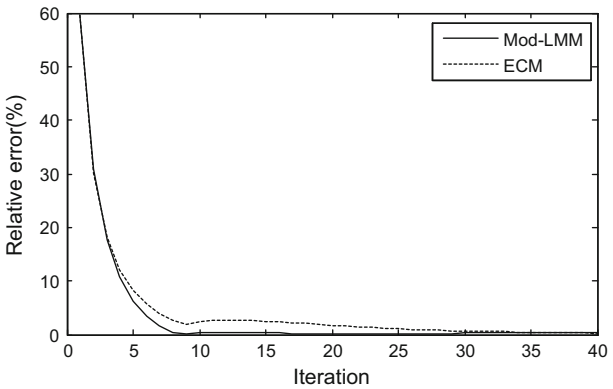

Fig. 4 Relative error of lower bound obtained using modified LMM and ECM as iterative process goes on

where $x = a/b$ [14,15].

Here, γ is equals to $2/\sqrt{3}$ for the von Mises yielding condition and $2/\sqrt{3}$ for the Tresca yielding condition, respectively.

According to Eq. (23), an analytical limit load factor is equals to 0.207 for this example. We computed the lower bound of limit load by using the LMM, the modified LMM and the ECM, respectively. Figure 8

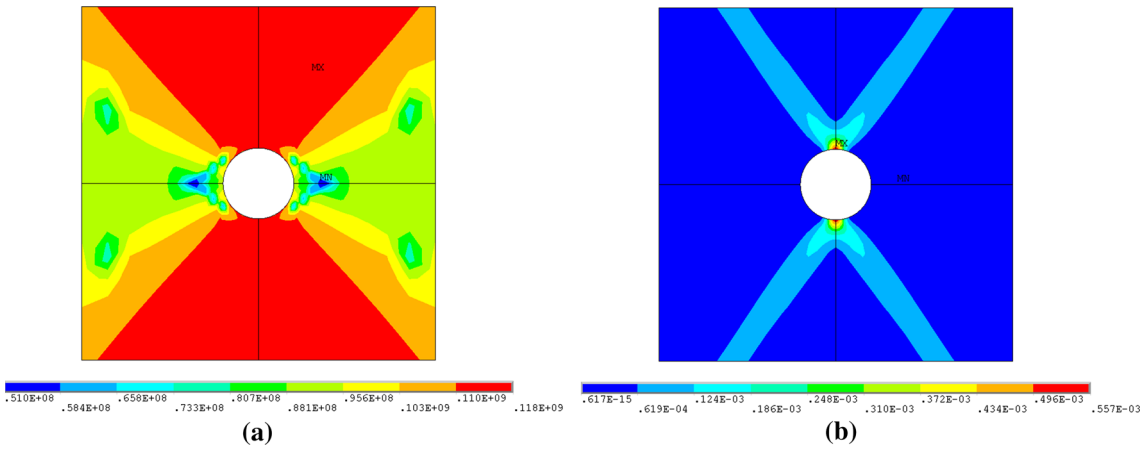

Fig. 5 Distribution of von Mises stress and equivalent strain evaluated at 40th iteration of modified LMM: **a** von Mises stress; **b** equivalent strain

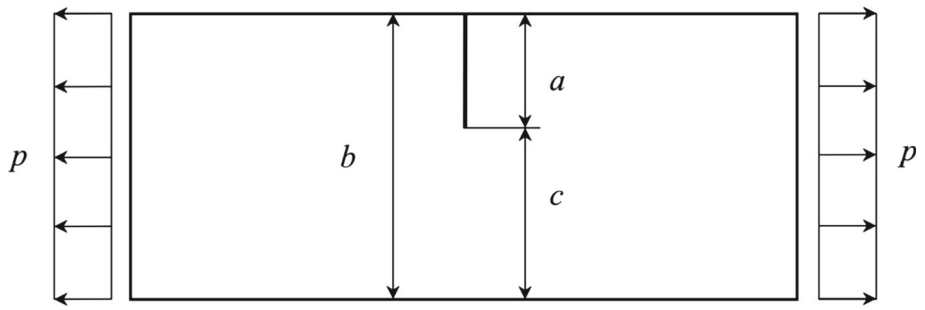

Fig. 6 Geometry of SE(T) specimen

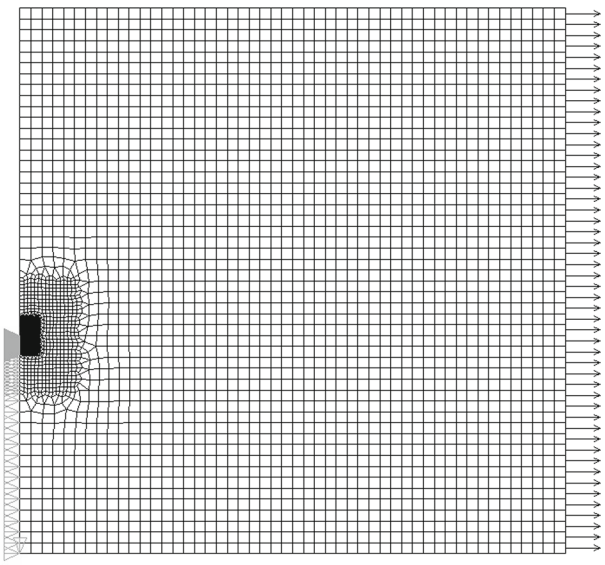

Fig. 7 FE mesh

compares the values of lower bound obtained using three different approaches as well as the upper bound as iterative process goes on.

As seen from Fig. 8, the values of lower bound evaluated using the LMM show the some numerical oscillations, while the convergence rate of ECM is slower than that of modified LMM even though it converges to the upper bound.

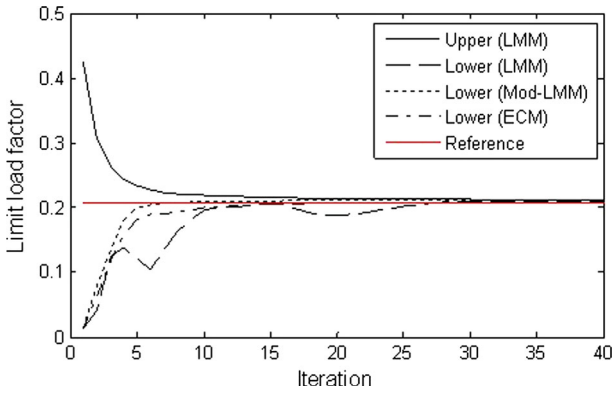

Fig. 8 Convergence process of *upper* and *lower* bound versus iteration number

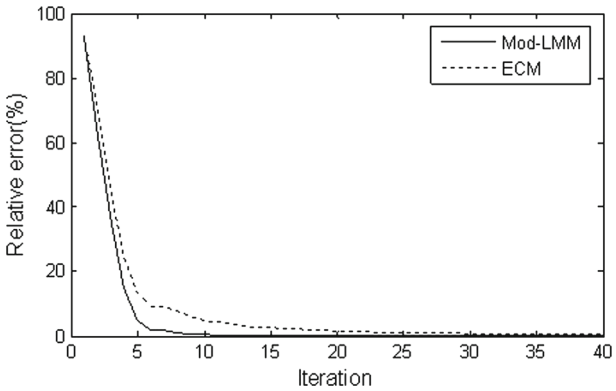

Fig. 9 Relative error of *lower* bound obtained using modified LMM and ECM versus iteration number

Due to numerical error of finite element analysis, we assume that the ECM is the reliable approach for the evaluation of lower bound and thus choose a value of 0.2096 obtained via 500 iterations of the ECM as a reference value of lower bound. Figure 9 shows the relative error of lower bound evaluated using the modified LMM and the ECM against the reference value, respectively. As shown from this figure, the LMM always yields the smaller relative error than the ECM for the evaluation of lower bound of limit load.

4.3 Axisymmetric pressure vessel subjected to the internal pressure

The axisymmetric pressure vessel is studied, which has been investigated by many researchers [16,17], as shown in Fig. 10. The geometrical dimension of $R_b = 4500\,\text{mm}$, $R_z = L = 3000\,\text{mm}$, $l = 658.2\,\text{mm}$, $R_k = 360\,\text{mm}$ and $s = 225\,\text{mm}$ is assumed, respectively.

For the internal pressure of $p = \sigma_y$, the limit load factor is found as $0.0746 \sim 0.083$ in Ref [16] and as 0.078 in Ref [17], respectively.

The FE model consists of 384 PLANE182 elements and 485 nodal points. B-bar Method (Selective Reduced Integration) and mixed u-p formulation are used.

Figure 11 depicts the convergence process of lower bound evaluated using three different approaches as well as upper bound. As seen from this figure, the evaluation of lower bound by the modified LMM has the best trend of convergence. A lower bound of 0.0783 was predicted via 500 iterations using the ECM. This value was taken as a reference value, and the relative error was compared based on this value as shown in Fig. 12.

4.4 Pipe-junction under internal pressure

The 3D pipe-junction subjected to the internal pressure is considered for limit analysis as shown in Fig. 13. The geometrical dimension of $D = 39\,\text{mm}$, $d = 15\,\text{mm}$ and $s = t = 3.4\,\text{mm}$ is assumed, respectively. For

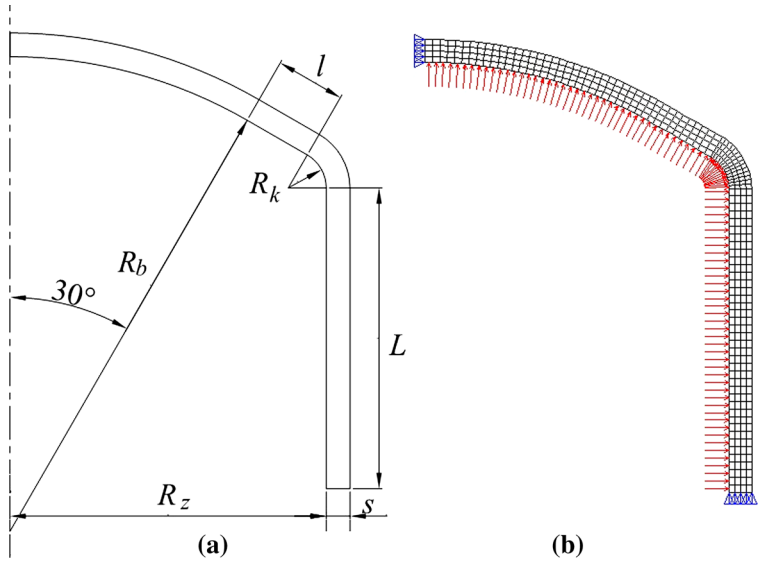

Fig. 10 **a** Geometry of pressure vessel; **b** FE mesh for limit analysis

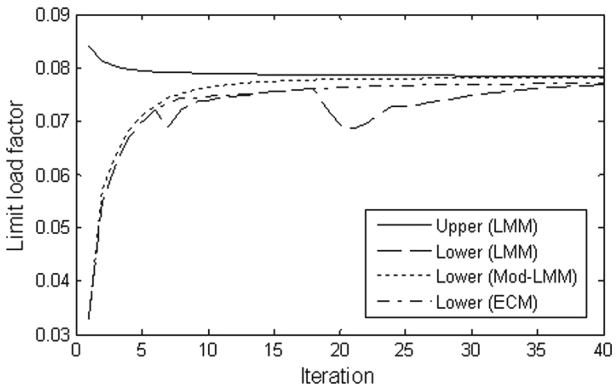

Fig. 11 Convergence process of *lower* bound and *upper* one versus iteration number

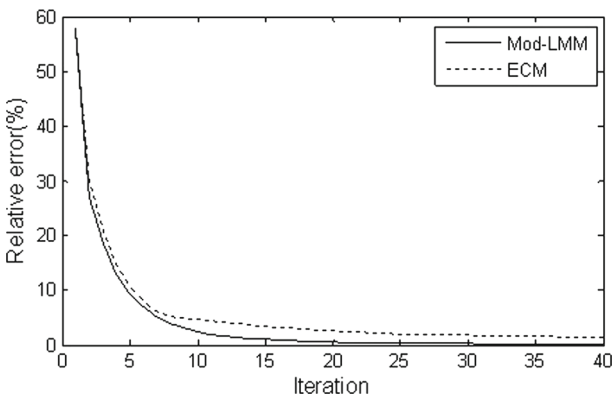

Fig. 12 Relative error of *lower* bound obtained using modified LMM and ECM versus iteration number

the internal pressure of $p = \sigma_y$, a limit load factor is known as 0.1443 in Ref. [17] and as 0.134 in Ref. [18], respectively.

The FE model consists of 2889 SOLID185 elements and 7037 nodal points. B-bar Method (Selective Reduced Integration) and mixed u-p formulation are used.

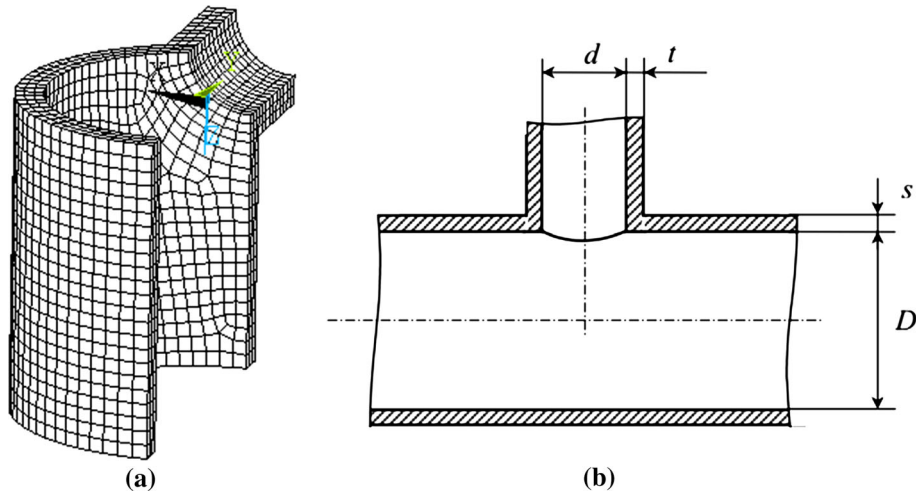

Fig. 13 **a** FE mesh for the limit analysis; **b** geometry of 3D pipe-junction

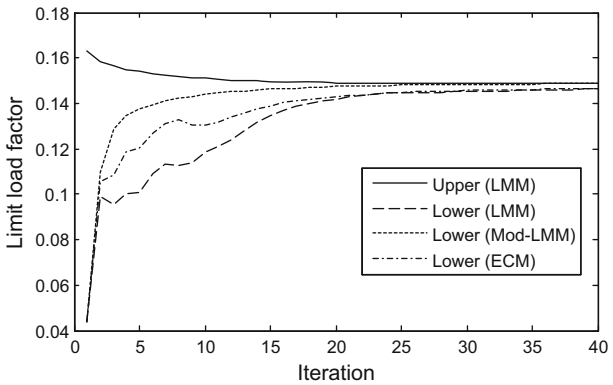

Fig. 14 Convergence process of limit load factor for 3D pipe-junction

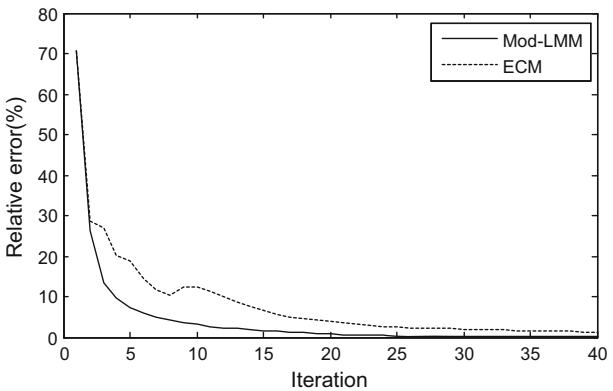

Fig. 15 Relative error of *lower* bound obtained using modified LMM and ECM versus iteration number

Figure 14 depicts the convergence process of upper bound and the lower one evaluated using three different approaches. As seen from Fig. 14, the evaluation of lower bound by the modified LMM has the best trend of convergence.

A lower bound of 0.1485 computed via 500 iterations using the ECM was used as the reference value for the comparison of relative error as shown in Fig. 15.

5 Conclusion

In this paper, we proposed a modified LMM and a newly defined lower bound for improving the convergence LMM. It was proved that this modified LMM never affects the numerical solution of lower and upper bounds of conventional LMM and that the newly evaluated lower bound satisfies the lower bound theorem and converges to the upper bound after sufficient numbers of iteration go on. Several numerical examples confirmed that the proposed algorithm is more accurate than other approaches. Moreover, our approach can effectively predict the upper bound as well as the lower one simultaneously only using LMM.

It should be noted that the current method can be applied effectively to the limit analysis of large scale problems in practice because it can be implemented using ANSYS UserMat and moreover the limit analysis is performed like the general elastic FEA in ANSYS.

Acknowledgements The authors would like to express their deep gratitude to Professor A.R.S Ponter of University of Leicester, UK, for valuable comments on this work.

References

1. Weichert, D., Ponter, A.R.S.: Limit states of materials and structures. Springer, Wien/New York (2009)
2. Simon, J.-W., Weichert, D.: Numerical lower bound shakedown analysis of engineering structures. Comput. Method Appl. Mech. Eng. **200**, 2828–2839 (2011)
3. Ponter, A.R.S., Carter, K.F.: Limit state solutions, based upon linear elastic solutions with a spatially varying elastic modulus. Comput. Method Appl. Mech. Eng. **140**, 237–258 (1997)
4. Ponter, A.R.S., Fuschi, P., Engelhardt, M.: Limit analysis for a general class of yield conditions. Eur. J. Mech. A Solid **19**, 401–421 (2000)
5. Chen, H.F., Ponter, A.R.S.: Shakedown and limit analyses for 3D structures using the linear matching method. Int. J. Press. Vessel Pip. **78**, 443–451 (2001)
6. Chen, H.F.: Lower and upper bound shakedown analysis of structures with temperature-dependent yield stress. J. Press. Vessel Tech. **132**, 1–8 (2010)
7. Chen, H.F.: Linear matching method for design limits in plasticity. Comp. Mat. Continua **20**, 159–183 (2010)
8. Barrera, O., Cocks, A.C.F., Ponter, A.R.S.: The linear matching method applied to composite materials: a micromechanical approach. Compos. Sci. Technol. **71**, 797–804 (2011)
9. Pisano, A.A., Fuschi, P.: A numerical approach for limit analysis of orthotropic composite laminates. Int. J. Numer. Method Eng. **70**, 71–93 (2007)
10. Pisano, A.A., Fuschi, P.: Mechanically fastened joints in composite laminates: evaluation of load bearing capacity. Compos. Part B Eng. **42**, 949–961 (2011)
11. Pisano, A.A., Fuschi, P., De Domenico, D.: Peak load prediction of multi-pin joints FRP laminates by limit analysis. Compos. Struct. **96**, 763–772 (2013)
12. Tipping, D.J.: The linear matching method: a guide to the ABAQUS user subroutines, Report E/REP/BBGB/0017/GEN/07, British Energy Generation Ltd, (2008)
13. Sadd, M.H.: Elasticity: theory, applications, and numerics. Elsevier Academic Press, Burlington (2005)
14. Ewing, D.J.F., Richards, C.E.: The yield-point loads of singly-notched pin loaded tensile strips. J. Mech. Phys. Solid **22**, 27–36 (1974)
15. Miller, A.G.: Review of limit loading of structures containing defects. Int. J. Press. Vessel. Pip. **32**, 197–327 (1988)
16. Yamamoto, Y., Asada, S., Okamoto, A.: Round robin calculations of collapse loads—a torispherical pressure vessel head with a conical transition. ASME. J. Press. Vessel. Tech. **119**, 503–509 (1997)
17. Khoi, V.D.: Dual limit and shakedown analysis of structures, PhD Thesis, Université de Liége, Belgium, (2001)
18. Staat, M., Heitzer, M.: Limit and shakedown analysis for plastic safety of complex structures. Transactions of the 14th international conference on structural mechanics in reactor technology (SMiRT 14), Vol. B, Lyon, France, August 17–22, B02/2 (1997)